ARTICLE

Check for updates

Effector memory CD4$^+$T cells in mesenteric lymph nodes mediate bone loss in food-allergic enteropathy model mice, creating IL-4 dominance

Aiko Ono-Ohmachi[1,2], Satoki Yamada[3], Satoru Uno[3], Masato Tamai[3], Kohei Soga[3], Shotaro Nakamura[3], Nobuyuki Udagawa[4], Yuko Nakamichi[5], Masanori Koide[5], Yoshikazu Morita[1], Tomohiro Takano[3], Takumi Itoh[6,7], Shigeru Kakuta[8], Chikao Morimoto[6], Shuji Matsuoka[9], Yoichiro Iwakura[10], Michio Tomura[11], Hiroshi Kiyono[12,13,14], Satoshi Hachimura[3] and Haruyo Nakajima-Adachi[3,12]✉

Intestinal inflammation can be accompanied by osteoporosis, but their relationship, mediated by immune responses, remains unclear. Here, we investigated a non-IgE-mediated food-allergic enteropathy model of ovalbumin (OVA) 23-3 mice expressing OVA-specific T-cell-receptor transgenes. Mesenteric lymph nodes (MLNs) and their pathogenic CD4$^+$T cells were important to enteropathy occurrence and exacerbation when the mice were fed an egg-white (EW) diet. EW-fed OVA23-3 mice also developed bone loss and increased CD44^{hi}CD62L^{lo}CD4$^+$T cells in the MLNs and bone marrow (BM); these changes were attenuated by MLN, but not spleen, resection. We fed an EW diet to F1 cross offspring from OVA23-3 mice and a mouse line expressing the photoconvertible protein KikGR to track MLN CD4$^+$T cells. Photoconverted MLN CD44^{hi}CD62L^{lo}CD4$^+$T cells migrated predominantly to the BM; pit formation assay proved their ability to promote bone damage via osteoclasts. Significantly greater expression of IL-4 mRNA in MLN CD44^{hi}CD62L^{lo}CD4$^+$T cells and bone was observed in EW-fed OVA23-3 mice. Anti-IL-4 monoclonal antibody injection canceled bone loss in the primary inflammation phase in EW-fed mice, but less so in the chronic phase. This novel report shows the specific inflammatory relationship, via Th2-dominant-OVA-specific T cells and IL-4 production, between MLNs and bone, a distant organ, in food-allergic enteropathy.

Mucosal Immunology (2021) 14:1335–1346; https://doi.org/10.1038/s41385-021-00434-2

INTRODUCTION

Intestinal inflammation, such as celiac disease with small intestinal inflammation, as well as inflammatory bowel disease (IBD)[1]—has been reported to have osteoporosis as a comorbidity. Aberrantly activated T cells may play important roles in bone loss after intestinal inflammation[2]. Previously, in a model of non-IgE-mediated gastrointestinal food-allergy model of ovalbumin (OVA) 23-3 mice, which expresses OVA-specific T-cell receptor (TCR) transgenes[3], we demonstrated bone loss development with increased numbers of activated CD4$^+$T cells in the bone marrow (BM)[4]. Enteropathy is induced in these mice simply by feeding an egg-white (EW) diet containing OVA[3]. This model shows typical allergic responses accompanied by weight loss and severe intestinal morphological changes, followed by intestinal infiltration by inflammatory cells (7 to 10 days' EW feeding, primary phase), and serum IgE production (14 days' EW feeding)[3,5]. Prolonged EW feeding (28 days, chronic phase) attenuates OVA-specific CD4$^+$T-cell activation and ameliorates the inflammation via regulatory T-cell (Treg) induction[5,6]. Despite these changes in the enteropathy pathology, bone loss seemed to be maintained during the experimental period[4]. As the enteropathy is triggered by MLNs and their aberrantly activated IL-4-producing MLN CD4$^+$T cells through food-allergen intake alone[5], bone loss in these mice may occur through allergen-specific immune responses activated and promoted in the MLNs. Allergic diseases (e.g., atopic dermatitis) may be associated with osteoporosis[7–9]. One potential mechanism reported from a study of *lck*-IL-4 transgenic mice is that continuous and excessive IL-4 production by activated T cells induces osteoporosis[10]. However, it remains unclear whether food-allergy-associated gastrointestinal inflammatory responses affect bone loss.

[1]Milk Science Research Institute, Megmilk Snow Brand Co., Ltd., Saitama, Japan. [2]Department of Quality Assurance, Bean Stalk Snow Co., Ltd., Tokyo, Japan. [3]Research Center for Food Safety, Graduate School of Agricultural and Life Sciences, The University of Tokyo, Tokyo, Japan. [4]Department of Biochemistry, Matsumoto Dental University, Nagano, Japan. [5]Institute for Oral Science, Matsumoto Dental University, Nagano, Japan. [6]Department of Therapy Development and Innovation for Immune Disorders and Cancers, Juntendo University, Tokyo, Japan. [7]Atopy (Allergy) Research Center, Graduate School of Medicine, Juntendo University, Tokyo, Japan. [8]Laboratory of Biomedical Science, Graduate School of Agricultural and Life Sciences, The University of Tokyo, Tokyo, Japan. [9]Department of Immunological Diagnosis, Graduate School of Medicine, Juntendo University, Tokyo, Japan. [10]Research Institute for Biomedical Sciences, Tokyo University of Science, Chiba, Japan. [11]Laboratory of Immunology, Faculty of Pharmacy, Osaka Ohtani University, Nishikiorikita, Tondabayashi-shi, Osaka, Japan. [12]IMSUT Distinguished Professor Unit, Division of Mucosal Immunology, The Institute of Medical Science, The University of Tokyo, Tokyo, Japan. [13]Mucosal Immunology and Allergy Therapeutics, Future Medicine Education and Research Organization, Institute for Global Prominent Research, Graduate School of Medicine, Chiba University, Chiba, Japan. [14]Division of Gastroenterology, Department of Medicine, School of Medicine, CU-UCSD Center for Mucosal Immunology, Allergy and Vaccines, University of California, San Diego, CA, USA. ✉email: haruyona@g.ecc.u-tokyo.ac.jp

Received: 6 August 2020 Revised: 7 June 2021 Accepted: 6 July 2021
Published online: 29 July 2021

We believed that, to clarify the mechanism by which food-allergic enteropathy induces the loss of bone—an extraintestinal organ—OVA23-3 mice were superior to other mouse models in terms of the technique used to alter their immunological condition, namely by simply feeding EW. We therefore analyzed this mouse model and discovered a specific relationship of the gut–bone axis via Th2-dependent immune responses between inflammatory MLNs and bone loss in food-allergic enteropathy.

RESULTS

EW feeding leads to bone loss in OVA23-3 mice

To minimize the influence of differences in nutrient consumption and body-weight changes on bone metabolism in EW-fed OVA23-3 mice, we conducted pair feeding, in which mice were maintained under the same food-consumption condition (apart from the difference in the protein source) during the experiment. Weight gain (Fig. 1a) and serum biomarker levels (Table S1) did not differ significantly among the four groups, although some EW-fed OVA23-3 mice lost weight and developed enteropathy during the experimental period (Fig. 1a). Serum 1,25-dihydroxyvitamin D_3 levels in EW-fed mice were significantly higher (OVA23-3, Fig. S1 left) than that in casein control diet (CN)-fed mice or the same as in the CN-fed mice (R23-3/BALB, Fig. S1 right) throughout the experimental period, showing the involvement of 1,25-dihydroxyvitamin D_3 in bone loss in our model was not clear. Severe bone loss—a significant decrease in the percentage change in the trabecular bone mineral content (BMC) compared with that in CN- or EW-fed BALB/cA (BALB) mice and CN-fed OVA23-3 mice—began in OVA23-3 mice on day 7 (primary phase; Fig. 1b, left), and significant decreases in cortical BMC started on day 21 of EW feeding (chronic phase; Fig. 1b, right). These bone losses continued to the end of the experiment. Continuing trabecular bone loss was further confirmed by examining other bone-morphologic parameters (bone volume per tissue volume [BV/TV] and BMC/TV, $P < 0.01$, EW-fed OVA23-3 mice vs. CN- or EW-fed BALB mice and CN-fed OVA23-3 mice; Fig. S2A). On day 56 (prolonged feeding of the EW diet), significant decreases in some parameters (BMC, BV/TV, BMC/TV, and trabecular number [Tb.N]) and an increase in trabecular separation (Tb.Sp) in EW-fed OVA23-3 mice were confirmed (Figs. 1c and S2B). These results clearly showed that feeding conditions and absorption alterations via intestinal inflammation were not major factors influencing the severe trabecular bone loss and inhibition of age-dependent increases in cortical bone thickness exhibited by EW-fed OVA23-3 mice.

Like EW-fed OVA23-3 mice, the inbred food-allergic enteropathy BALB mouse model established by EW feeding after sensitization with OVA and alum (BALB/ALUM mice) showed enteropathy, recovery from inflammation[11], and bone loss (Fig. S3). Thus, our model's bone loss did not result from the presence of the TCR transgene but from the food-allergic enteropathy.

Aberrant OVA-specific CD44^{hi}CD62L^{lo}CD4^{+}T-cell activation induced in MLNs and BM by EW feeding triggers bone loss in EW-fed OVA23-3 mice

EW-fed, but not CN-fed, OVA23-3 mice deficient in recombination-activating gene (RAG) 2 mice (R23-3 mice) also showed significant weight loss (Fig. S4A) (a sign of enteropathy induced by IL-4-producing OVA-specific CD4^{+}T cells)[6] and bone loss as a comorbidity. Compared with CN-fed R23-3 mice, the EW-fed mice also had significant decreases in trabecular BMC (Fig. S4B, C), BV/TV, BMC/TV, and Tb.N and a significant increase in Tb.Sp (Fig. S5). In contrast, EW-fed Th1-type RAG-2-deficient D10 mice (RD10 mice)—another strain with OVA-TCR transgenes[6,12]—did not show weight loss or bone loss (Figs. S4 and S5)[6]. Therefore, aberrant activation of Th2-type OVA-specific CD4^{+}T-cells, inducing enteropathy, likely plays an important role in inducing bone loss. In contrast, OVA-specific B cells were not involved, because R23-3 mice developed bone loss despite lacking B cells. We confirmed the above possibility by establishing a model of transfer of OVA-specific MLN CD4^{+}T cells from R23-3 mice into severe combined immunodeficiency mice (SR23-3 mice). Only the EW-fed SR23-3 mice showed significant decreases in BMC and weight (Fig. S6, Results in the Supplementary Information).

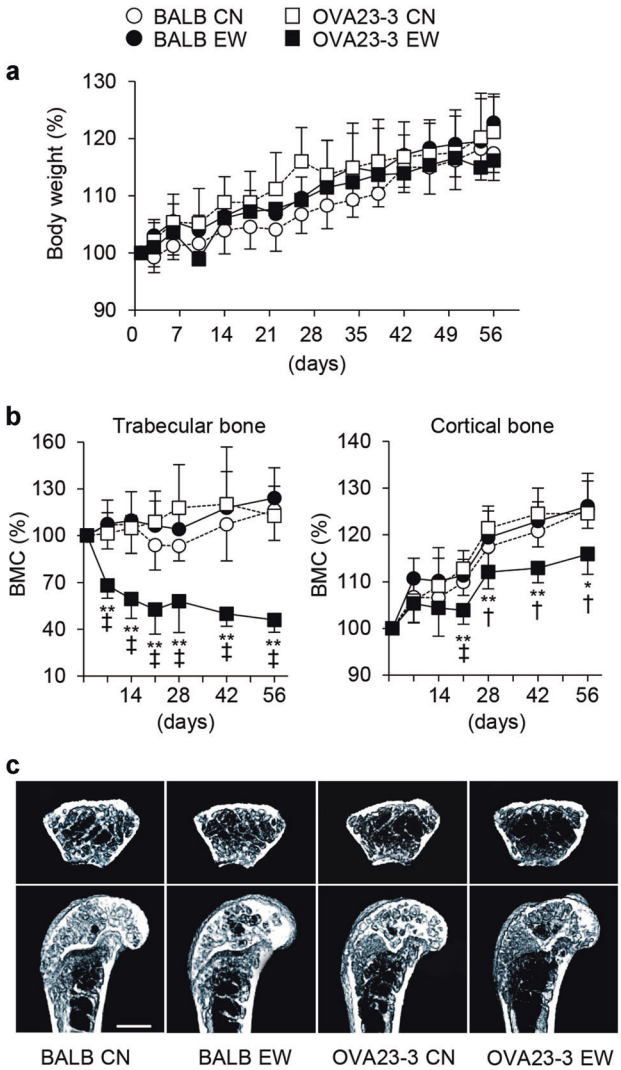

Fig. 1 Egg-white (EW)-fed OVA23-3 mice display bone loss. BALB mice and OVA23-3 mice were fed a control (CN) or EW diet for 56 days. **a** Time course of body-weight relative to initial values (100%). Initial body weights were: for BALB CN, 24 ± 0.99 g; BALB EW, 24.57 ± 0.73 g; OVA23-3 CN, 24.76 ± 1.94 g; OVA23-3 EW 24.99 ± 1.90 g. Body-weight was measured every 2 or 3 days. **b** Time courses of bone mineral content (BMC) in trabecular (left panel) and cortical (right panel) bone relative to initial values (100%). BMC was measured by using micro-computed tomography throughout the 56 days. BALB CN, CN-fed BALB mice (open circle (○)); BALB EW, EW-fed BALB mice (closed circle (●)); OVA23-3 CN, CN-fed OVA23-3 mice (open square (□)); OVA23-3 EW, EW-fed OVA23-3 mice (closed square (■)). **c** Computed tomography images of the distal femur after 56 days of CN or EW diets. Scale bar = 1 mm. $n = 3$ to 5 in each group. Data are representative of two independent experiments. $^{*}P < 0.05$ and $^{**}P < 0.01$ (OVA23-3 EW vs. BALB CN and OVA23-3 CN); $^{\dagger}P < 0.05$ and $^{\ddagger}P < 0.01$ (OVA23-3 EW vs. BALB EW).

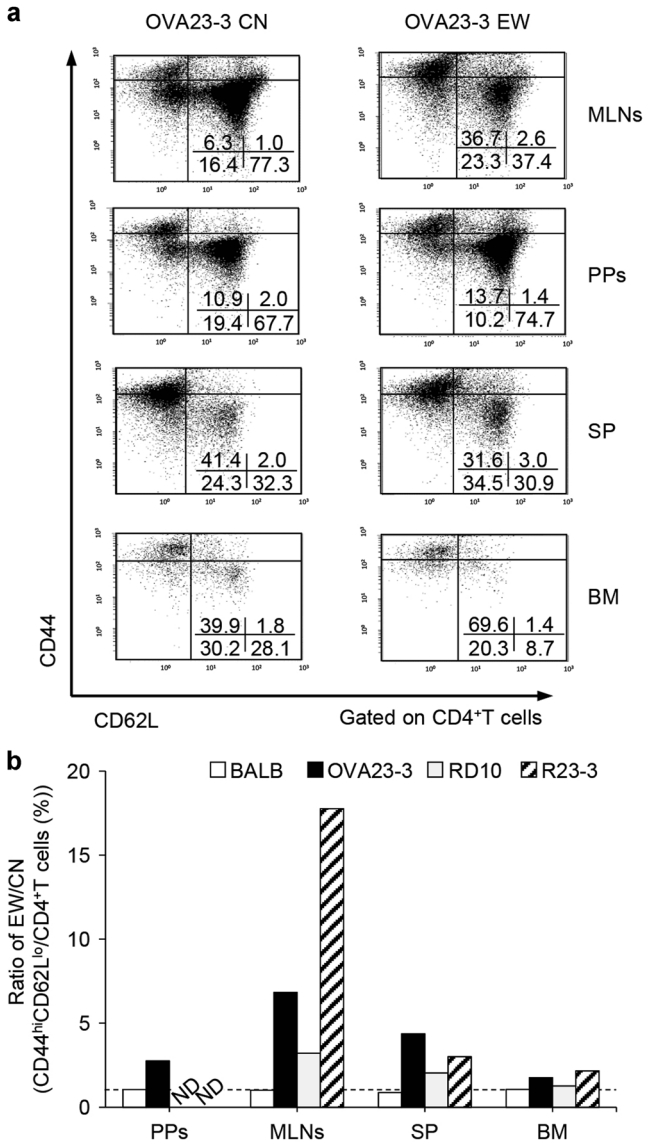

Fig. 2 Egg-white (EW) feeding induces CD44^{hi}CD62L^{lo}CD4^{+}T cells in OVA23-3 mice throughout the experimental period. Single-cell suspensions were prepared from mesenteric lymph nodes (MLNs), Peyer's patches (PPs), spleen (SP), and bone marrow (BM) of BALB, OVA23-3, R23-3, and RD10 mice fed a control (CN) or EW diet for 56 days. **a** Dot plots represent CD44 vs. CD62L gated on magnetic-activated-cell-sorting-separated CD4^{+}T cells of MLNs, PPs, SP, and BM in OVA23-3 mice fed a CN diet (left) or EW diet (right). Numbers in the plots indicate CD44^{hi}CD62L^{lo}CD4^{+}T cells and CD44^{hi}CD62L^{hi}CD4^{+}T cells (top row, left and right, respectively) and CD44^{int}CD62L^{lo}CD4^{+}T cells and CD44^{int}CD62L^{hi}CD4^{+}T cells (bottom row, left and right, respectively) as percentages of the total number of CD4^{+}T cells. **b** Each column indicates the ratio in EW-fed mice (BALB, OVA23-3, R23-3, and RD10) to that in CN-fed mice of CD44^{hi}CD62L^{lo}CD4^{+}T cells as a percentage of total CD4^{+}T cells from different lymphoid tissues (MLNs, PPs, SP, and BM). Dashed lines indicate a ratio of 1. The data were obtained by mixing cells from three mice in the CN or EW group and average of two independent experiments. ND = not detected.

Memory-phenotype CD4^{+}T cells maintained in the BM contribute to persistent IBD, with bone loss as a comorbidity[13–15]. To clarify the roles of CD44^{hi}CD62L^{lo}CD4^{+}T cells [effector-memory (EM) phenotype], which preferentially reside in BM[16–18], we measured CD44 and CD62L molecule expression on aberrantly activated CD4^{+}T cells in MLNs, spleen, Peyer's patches (PPs), and BM of EW- or CN-fed OVA23-3 mice. The proportions of these cells increased after EW feeding in OVA23-3 mice (Fig. 2a)—markedly so in MLNs (to about seven times that in CN-fed OVA23-3 mice) but also in the other tissues (to about two to four times those in CN-fed mice) (Fig. 2b). The proportion and number of CD44^{hi}CD62L^{lo} cells among MLN CD4^{+}T cells increased throughout EW feeding (Fig. S7A, B(a)). In MLNs, similar results were obtained in EW-fed R23-3 mice (to 18 times that in CN-fed R23-3 mice), whereas the increase in the proportion in EW-fed RD10 mice was smaller (triple that in CN-fed RD10 mice) (Fig. 2b). Residency of EM T cells in BM[16–18] was supported by our finding them there in CN-fed OVA23-3 mice (Fig. 2a); their proportion was enhanced after EW feeding. (to 1.7 times that in CN-fed OVA23-3 mice, Fig. 2b). EW feeding induced greater RANKL expression on the surfaces of CD62L^{lo}CD4^{+}T cells in MLNs and BM than in the spleen or PPs (Fig. S8A). RANKL expression in MLNs was enhanced time dependently (Fig. S7B(b), C); more than 95% of RANKL^{+}CD4^{+}T cells were of the CD44^{hi}CD62L^{lo} phenotype in EW-fed OVA23-3 mice (Fig. S8B). As RANKL can stimulate osteoclast differentiation[19], our results suggest that MLNs are a source of RANKL^{+}CD44^{hi}CD62L^{lo}CD4^{+}T cells for BM, with associated bone-loss induction, as indicated in different enteropathy models. (For details, see Fig. S9 and Results in the Supplementary Information).

MLNs, but not spleen, are important to bone-loss induction upon EW feeding

MLNs are essential to enteropathy development and as a source of aberrantly activated OVA-specific CD4^{+}T cells in EW-fed OVA23-3 mice[5]. To clarify the roles of MLNs in bone loss, we performed mesenteric lymphadenectomy or splenectomy on OVA23-3 mice, followed by EW feeding. On day 28 of EW feeding, in MLN-ectomized mice, the decreases in weight (Fig. S10A) and in trabecular (Fig. 3a, left) and cortical (Fig. 3a, right) BMC seen in MLN-sham-operated mice were mitigated significantly (weight loss, $P < 0.01$; trabecular BMC decrease, $P < 0.05$; cortical BMC decrease, $P < 0.05$; EW-fed MLN-ectomized vs. EW-fed MLN-sham-operated mice). In contrast, with EW feeding, splenectomy alleviated neither the weight loss (Fig. S10B) nor the BMC decrease (Fig. 3b) induced in spleen-sham-operated mice.

BM numbers of CD44^{hi}CD62L^{lo}CD4^{+}T cells and RANKL^{+}CD44^{hi}CD62L^{lo}CD4^{+}T cells were significantly lower in EW-fed MLN-ectomized mice than in EW-fed MLN-sham-operated mice ($P < 0.01$, Fig. 3c; $P < 0.05$, Fig. 3e, respectively). Spleen numbers of both cell types were significantly greater in EW-fed MLN-ectomized mice than in EW-fed MLN-sham-operated mice ($P < 0.05$, Fig. 3c, e); in PPs, there were no significant differences between these two groups, suggesting that the spleen changes occurring with the intestinal immune response were unrelated to those in the BM. There were no significant differences in BM numbers of either cell type between EW-fed splenectomized and spleen-sham-operated mice (Fig. 3d, f). These results clearly indicate that MLNs, but not the spleen, are important for bone-loss induction in food-allergic enteropathy. Moreover, MLN CD44^{hi}CD62L^{lo}CD4^{+}T-cell activation may be associated with BM immune responses in EW-fed OVA23-3 mice.

CD44^{hi}CD62L^{lo}CD4^{+}T cells in MLNs promote bone damage via osteoclasts independently of cell-surface RANKL expression

We isolated RANKL$^{+/-}$CD44^{hi}CD62L^{lo}CD4^{+}T cells, CD44^{int}CD62L^{lo}CD4^{+}T cells, and CD44^{int}CD62L^{hi}CD4^{+}T cells from MLNs of EW-fed or CN-fed OVA23-3 mice (Fig. 4a) and conducted pit-formation assays by adding these cells to preosteoclasts. Pit area, which reflects bone damage (osteoclast differentiation and bone resorption)-promoting ability via osteoclasts, was significantly greater in

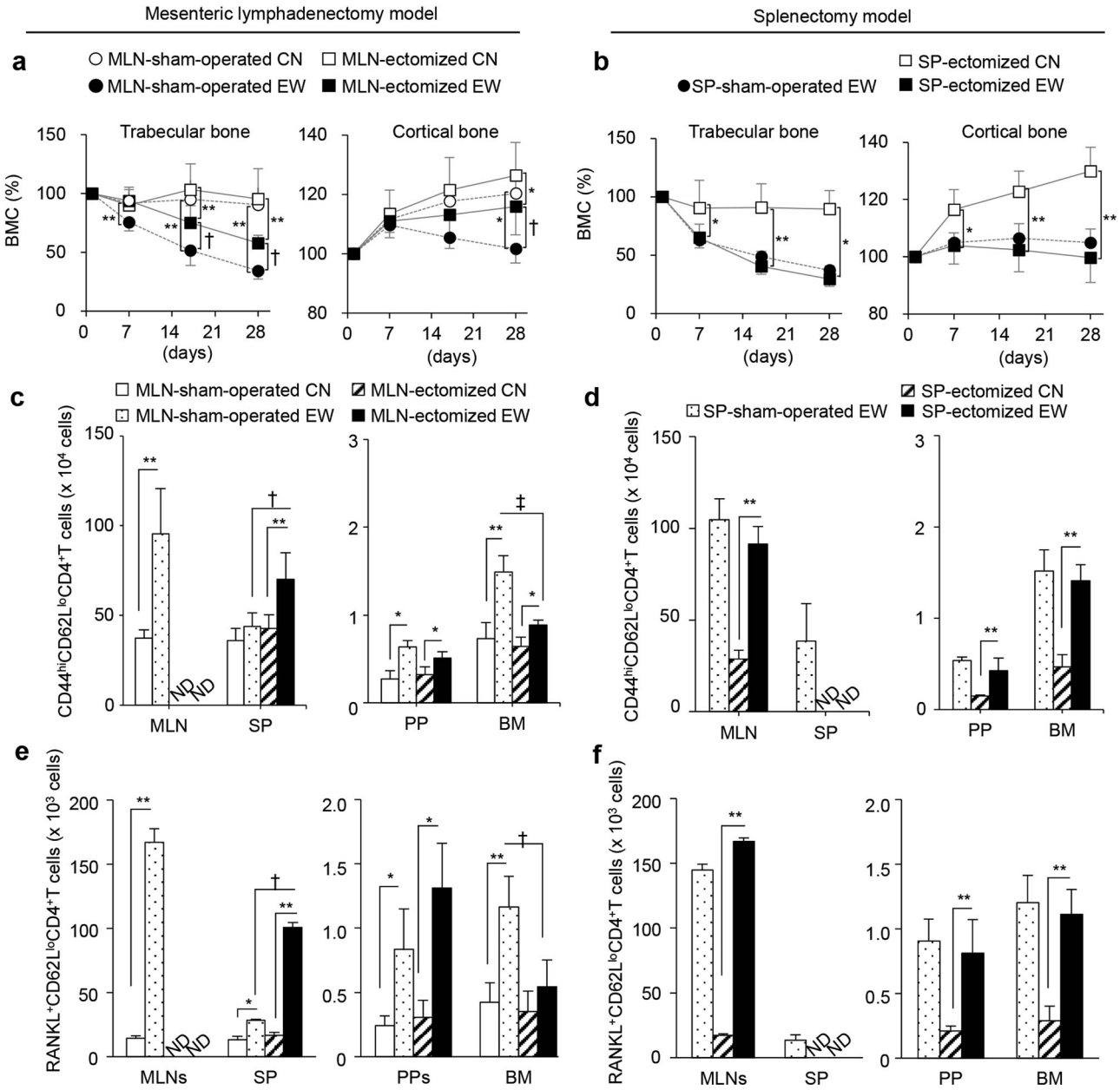

Fig. 3 Mesenteric lymph nodes (MLNs), but not the spleen (SP), play an important role in the bone loss induced by egg-white (EW)-fed OVA23-3 mice. Mesenteric lymphadenectomized (MLN-ectomized), MLN-sham-operated, splenectomized (SP-ectomized), and SP-sham-operated OVA23-3 mice were fed a control (CN) or EW diet for 28 days. Panels show time courses of bone mineral content (BMC) relative to initial values (100%) in trabecular (left) and cortical bone (right) after **a** mesenteric lymphadenectomy or **b** splenectomy. The numbers of $CD44^{hi}CD62L^{lo}CD4^{+}$T cells from different tissues (MLNs, Peyer's patches [PPs], spleen, and bone marrow [BM]) are shown after **c** mesenteric lymphadenectomy or **d** splenectomy. The numbers of $RANKL^{+}CD62L^{lo}CD4^{+}$T cells from different tissues are shown after **e** mesenteric lymphadenectomy or **f** splenectomy. MLN-sham-operated CN, CN-fed MLN-sham-operated OVA23-3 mice; MLN-sham-operated EW or SP-sham-operated EW, EW-fed MLN- or SP-sham-operated OVA23-3 mice; MLN-ectomized CN or SP-ectomized CN, CN-fed MLN- or SP-ectomized OVA23-3 mice; MLN-ectomized EW or SP-ectomized EW, EW-fed MLN- or SP-ectomized OVA23-3 mice; $n = 3$ to 5 in each group. Data are representative of two independent experiments. ND = not detected. $^{*}P < 0.05$ and $^{**}P < 0.01$ (EW vs. CN); $^{\dagger}P < 0.05$ and $^{\ddagger}P < 0.01$ (MLN-ectomized vs. MLN-sham-operated).

the presence of $RANKL^{+}$ or $RANKL^{-}CD44^{hi}CD62L^{lo}CD4^{+}$T cells isolated from EW-fed OVA23-3 mice than in the presence of these cells isolated from CN-fed OVA23-3 mice ($P < 0.01$, Fig. 4b, c). In contrast, $RANKL^{-}CD44^{int}CD62L^{lo}CD4^{+}$T cells from either CN- or EW-fed OVA23-3 mice suppressed bone-damage-promoting ability via osteoclasts (Fig. 4b, c). Notably, in this culture, stimulating preosteoclasts with $CD44^{hi}CD62L^{lo}CD4^{+}$T cells without adding soluble RANKL did not induce the in vitro differentiation of tartrate-resistant acid phosphatase-positive ($TRAP^{+}$) multinucleated cells (i.e., there were no osteoclasts) (Fig. S11). These results indicated that (1) MLN $CD44^{hi}CD62L^{lo}CD4^{+}$T cells activated by EW feeding promoted bone damage, which was independent of T-cell-surface RANKL expression; and (2) $CD44^{hi}CD62L^{lo}CD4^{+}$T cells, but not naive $CD4^{+}$T cells or $CD44^{int}CD62L^{lo}CD4^{+}$T cells (which suppress bone damage), in MLNs induced bone damage in EW-fed OVA23-3 mice.

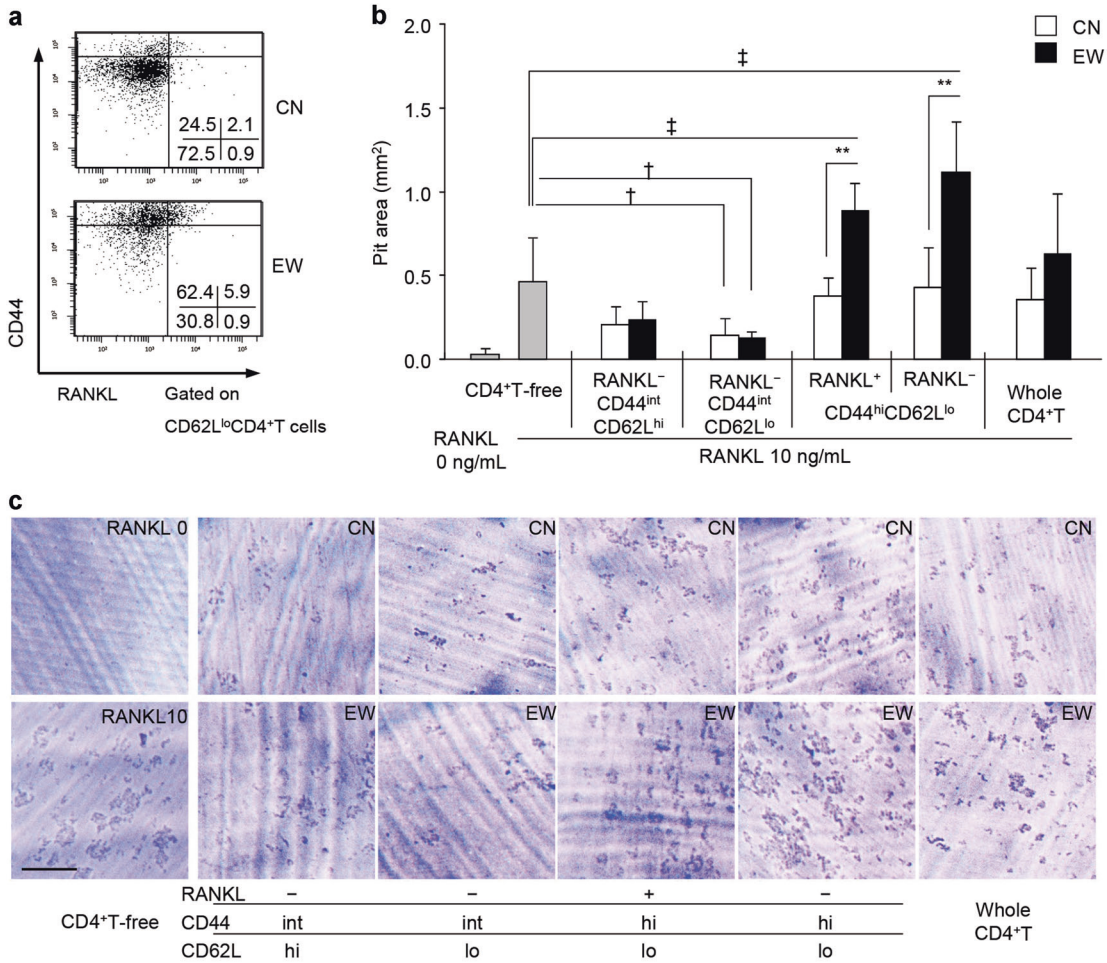

Fig. 4 CD44^{hi}CD62L^{lo}CD4^{+}T cells promote bone damage independently of receptor activator of nuclear factor kappa-B ligand (RANKL) expression. The bone-resorption effects of each CD4^{+}T-cell subset purified from mesenteric lymph nodes (MLNs) of OVA23-3 mice after 28 days' feeding of control (CN) or egg-white (EW) diet were assessed by pit-formation activity. **a** Plots represent CD44 vs. RANKL gated on MLN CD62L^{lo}CD4^{+}T cells separated by using a BD FACS Aria II Cell Sorter. Each number in the panel indicates the number of cells in the corresponding quadrant as a percentage of all CD62L^{lo}CD4^{+}T cells. **b** White columns indicate cells derived from control diet (CN)-fed OVA23-3 mice, black columns represent cells derived from EW-fed OVA23-3 mice, and gray columns indicate CD4^{+}T-cell-free solution; the treatment was soluble RANKL (RANKL, 0 or 10 ng/mL), $n = 3$ to 10 for each column. $^{**}P < 0.01$ (EW vs. CN); $^{\dagger}P < 0.05$ and $^{\ddagger}P < 0.01$ (CD4^{+}T-cell subsets vs. CD4^{+}T cell-free, treated with 10 ng/mL RANKL). **c** Stereo-microscopic images of representative resorption pits. Resorption pits appear as darkly stained areas. + or −, positive or negative expression of RANKL molecule on CD4^{+}T-cell surface. Scale bar = 500 μm.

MLN CD44^{hi}CD62L^{lo}CD4^{+}T cells migrate preferentially to the BM

To examine whether OVA-activated MLN CD4^{+}T cells directly migrated to BM, we generated K23-3 mice from a cross between Kikume Green-Red (KikGR) mice[20] and OVA23-3 mice. Using KikGR mice allowed us to pinpoint the original tissue (i.e., MLN) of cells migrating to BM more precisely than with standard techniques such as adoptive transfer of carboxyfluorescein-succinimidyl-ester-labeled cells. Violet-light exposure of MLNs revealed that over 80% of all MLN cells photoconverted from green to red (Fig. 5a). After 10 days of EW feeding, K23-3 mice, like EW-fed OVA23-3 mice, exhibited enteropathy with weight loss (Fig. 5b, c) and bone loss (Fig. 5d). To analyze the influence of EW feeding on cell migration, MLNs of EW-fed K23-3 mice were exposed to violet light on day 9 (Fig. 5e). We then euthanized the mice and quantified the CD44^{hi}CD62L^{lo} cells as a percentage of the total number of KikGR-red CD4^{+}T cells in each tissue on day 10 (Fig. S12). In CN-fed K23-3 mice, MLN CD4^{+}T cells migrated to BM (3–6% of KikGR-red CD4^{+}T cells); migration was increased significantly by EW feeding (25–33% of KikGR-red CD4^{+}T cells; $P < 0.01$, Figs. 5f and S12). Interestingly, the percentage of KikGR-red-converted CD44^{hi}CD62L^{lo}CD4^{+}T cells in EW-fed K23-3 mice was greater in BM than in MLNs, spleen, and skin-draining lymph nodes (sDLNs) (Fig. 5f). In MLNs, no difference was observed between EW- and CN-fed K23-3 mice in CD44^{hi}CD62L^{lo}CD4^{+}T cells as a percentage of the total number of KikGR-red CD4^{+}T cells (Fig. 5f) or in RANKL^{+}cells as a percentage of the total number of KikGR-red CD44^{hi}CD62L^{lo}CD4^{+}T cells (Fig. S9E), indicating that CD44^{hi}CD62L^{lo}CD4^{+}T cells tended to stay in MLNs during inflammation, probably to respond to invasion by allergens. Therefore, although CD44^{hi}CD62L^{lo}CD4^{+}T cells can migrate easily to BM, even with control feeding, the enteropathy induced by EW feeding promotes migration of these cells from MLNs to BM once they leave the MLNs and enter the circulation.

IL-4 predominates in both intestine and bone of EW-fed OVA23-3 mice

In studies analyzing cytokine mRNA expression, we concluded that IL-4 and IL-1β,—but not IL-6 and TNF-α—were representative cytokines produced by whole cells from each lymphoid organ in our model (Fig. S13). IL-17 was analyzed because exFoxpTh17 cells were reported to induce bone loss[21–24]. On day 9 of severe inflammation from EW feeding, intestinal IL-4 mRNA expression was significantly greater in EW-fed OVA23-3 mice than in CN-fed mice; in the bone, levels of both IL-1β and IL-4 were significantly

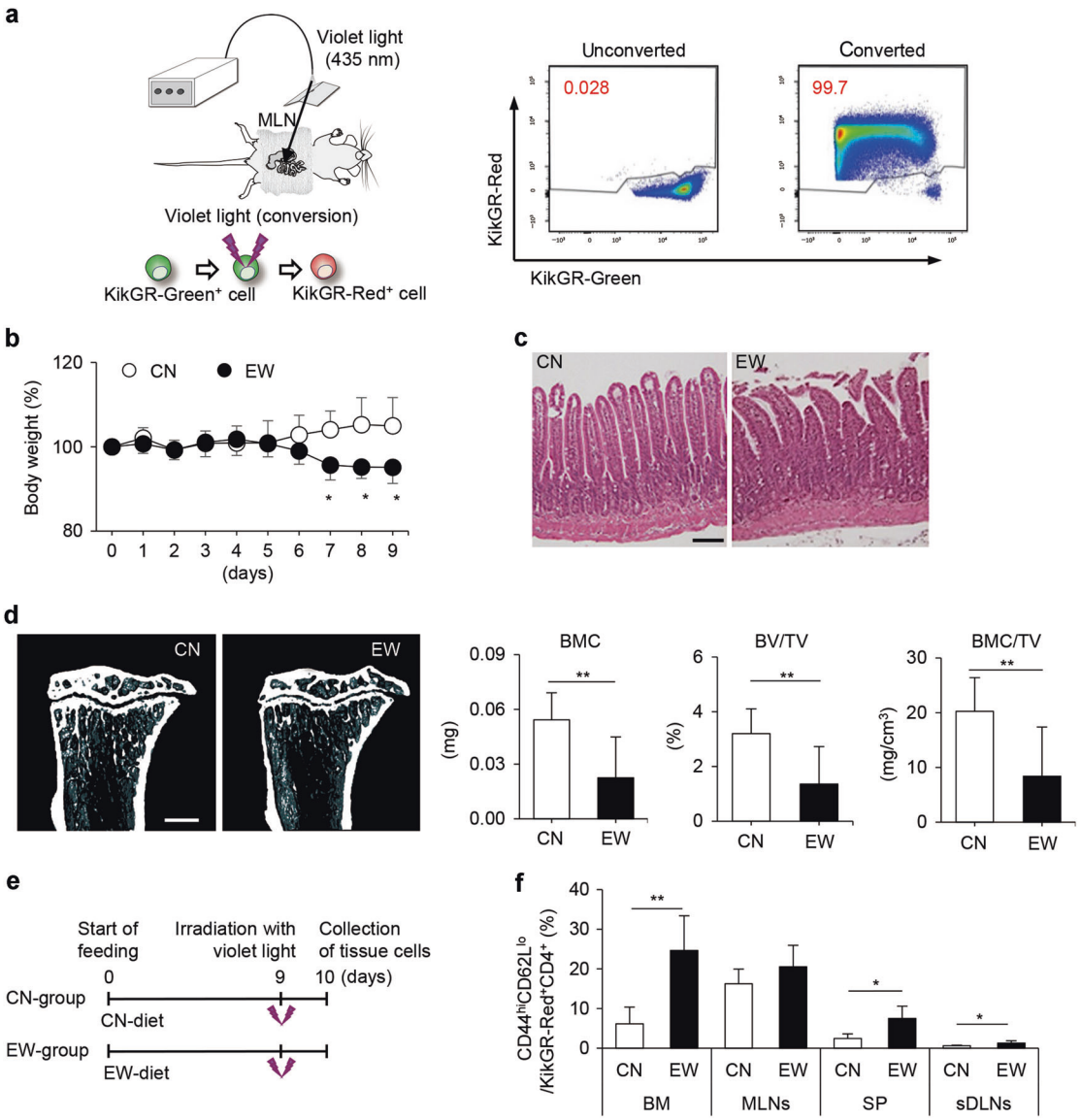

Fig. 5 Egg-white (EW) feeding promotes weight loss, intestinal changes, bone loss, and migration of CD44^{hi}CD62L^{lo}CD4^{+}T cells from mesenteric lymph nodes (MLNs) to bone marrow (BM) in K23-3 mice. a Photoconversion method by irradiation of MLNs with violet light (left). Representative plots (right) of KikGR-green and -red MLN cells of K23-3 mice. The number in each plot indicates KikGR-red cells as a percentage of the total MLN cells. **b** Time course of body-weight relative to initial weight (100%). Initial body-weight of CN-fed K23-3 mice was 28.06 ± 3.42 g and that of EW-fed K23-3 mice was 28.47 ± 1.82 g. **c** Hematoxylin and eosin-stained paraffin-embedded small intestinal tissues (4 μm thick). Scale bar = 100 μm. **d** Right tibia scanned by micro-computed tomography (left). Scale bar = 1 mm. Trabecular bone mineral content (BMC), bone volume per tissue volume (BV/TV), and bone mineral content per tissue volume (BMC/TV) of the tibia (right). **e** Protocol of EW feeding and irradiation of MLNs with violet light. **f** CD44^{hi}CD62L^{lo}CD4^{+}T cells as a percentage of the total KikGR-red-positive CD4^{+}T cells from bone marrow (BM), MLNs, spleen (SP), and skin-draining lymph nodes (sDLNs) of K23-3 mice. Values are expressed as means ± SD. CN-fed K23-3 mice, $n = 4$ to 6; EW-fed K23-3 mice, $n = 6$ to 9. Results are representative of two independent experiments. *$P < 0.05$ and **$P < 0.01$ (EW vs. CN).

greater in EW-fed OVA23-3 mice (Fig. 6a). IL-17 expression was detected in bone even in CN-fed OVA23-3 mice, but it was decreased significantly by EW feeding (Fig. 6a). On day 9 of severe inflammation in EW-fed OVA23-3 mice, the cytokine expression patterns in MLN CD4^{+}T cells and MLNs, spleen, and BM whole cells were similar to those in intestine or bone (Fig. 6b). After EW feeding, expression levels of IL-4—but not IL-5 and IL-13 (other Th2 cytokines of allergic responses)—significantly increased and IL-1β predominated in BM cells, but IL-17 mRNA expression levels were similar to those in the CN groups, with the exception of a significant decrease in expression in MLN CD4^{+}T cells (Fig. 6b). Significantly higher IL-4 mRNA expression levels were observed in KikGR-red cells sorted from BM of K23-3 mice fed EW for 9 days than in those from CN-fed mice. In contrast, levels of CXCR4 mRNA were significantly lower in the EW-fed mice (Fig. S14), suggesting that MLN cells migrated, probably in response to CXCL12 (a ligand for CXCR4) produced in BM, and together with resident BM cells produced IL-4[25,26].

In activated MLN CD44^{hi}CD62L^{lo}CD4^{+}T cells and other MLN CD4^{+}T-cell subsets of OVA23-3 mice on day 28 of EW feeding, when severe bone loss was observed, although there were insufficient RANKL^{+}CD44^{hi}CD62L^{lo}CD4^{+}T cells from CN-fed OVA23-3 mice for analysis [shown as "not detected (ND)" (Fig. 7a)], high IL-4 mRNA expression levels in RANKL^{+}CD44^{hi}CD62L^{lo}CD4^{+}T cells and whole CD4^{+}T cells were detected in EW-fed OVA23-3 mice. However, IL-17 and IL-1β mRNA expression levels were not greater than those in

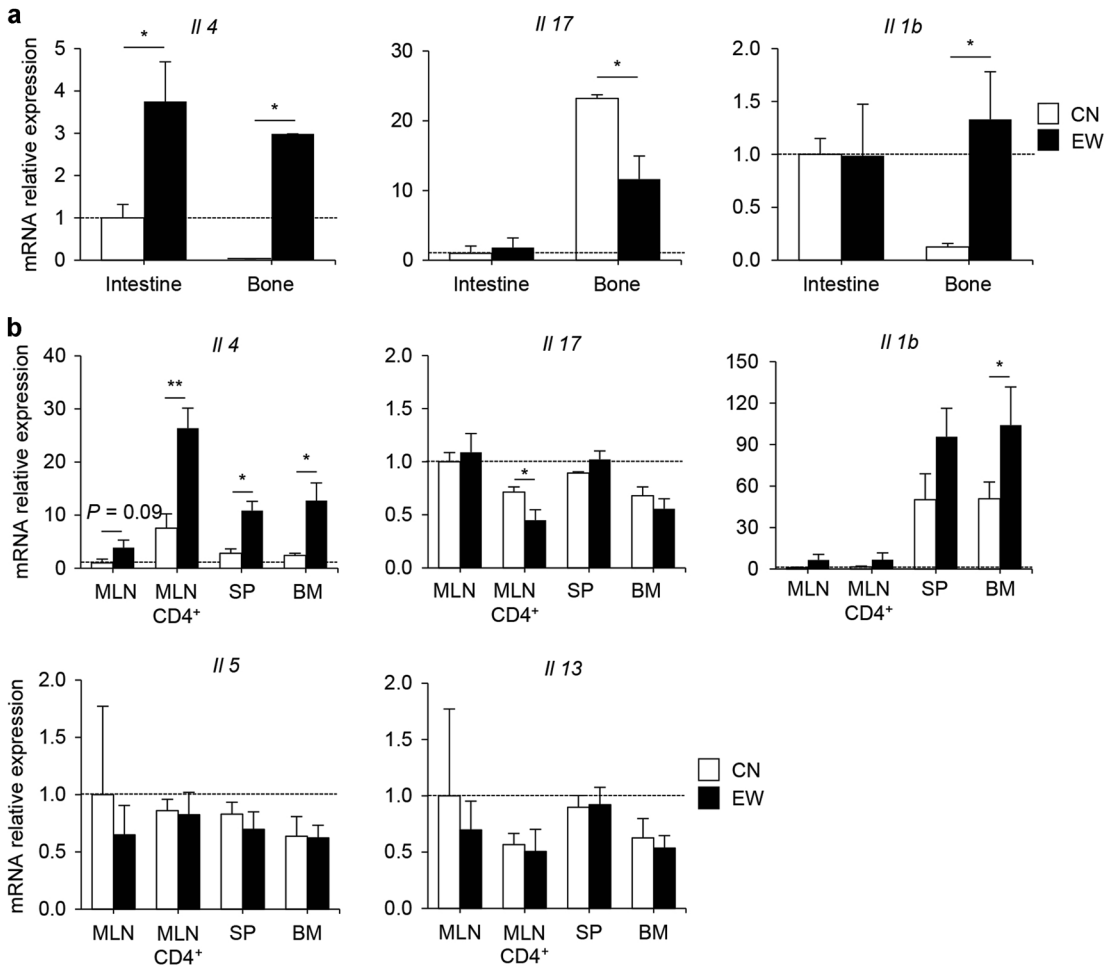

Fig. 6 Analysis of cytokine mRNA expression patterns in egg-white (EW)-fed OVA23-3 mice shows predominant IL-4 and IL-1β production. OVA23-3 mice were fed a control (CN) or EW diet for 9 days. Organs or tissues (intestine or bone) and lymphocytes (from mesenteric lymph nodes [MLNs], spleen [SP], or bone marrow [BM], or MLN $CD4^+$T cells) were examined for cytokine mRNA expression at the end of EW feeding (day 9). Cytokine mRNA expression levels were determined by Quantitative real-time RT-PCR and are shown relative to the values in the intestine or MLN cells of CN-fed mice (horizontal line) for **a** intestine and bone, and **b** MLNs and MLN $CD4^+$T, SP, and BM cells. (open square (□)) CN-fed group, $n = 3$; (closed square (■)) EW-fed group, $n = 3$. Data are representative of two independent experiments. $^*P < 0.05$ and $^{**}P < 0.01$ (EW vs. CN).

CN-fed OVA23-3 mice (Fig. 7a). In MLN cells of OVA23-3 mice on day 28 of EW feeding, the expression level of IL-4—but not IL-1β and IL-17—mRNA was also significantly enhanced (Fig. 7b). Thus, activated IL-4-producing MLN $CD44^{hi}CD62L^{lo}CD4^+$T cells may help create IL-4 dominance, as suggested by the increased numbers of multi-nucleated inflammatory cells (neutrophils and eosinophils) in BM (Fig. S15).

Primary, but not chronic-phase, IL-4 production is critical for inducing bone loss in food-allergic enteropathy

F1 R23-3/BALB mice were injected intravenously with anti-IL-4 monoclonal antibody (αIL-4 mAb) before diet feeding and on day 7 (Fig. 8a). Weight loss (Fig. 8b), enteropathy (Fig. 8c), and bone loss (Fig. 8d) were relieved by αIL-4 mAb injection. Bone parameters (BMC, BV/TV, and BMC/TV) had recovered significantly in EW-fed αIL-4 mAb-injected mice by 9 days ($P < 0.05$, Fig. 8e). Mice injected with αIL-4 mAb on days 10, 17, and 24 of EW feeding (Fig. 8g) had earlier weight loss recovery and less enteropathy than control Ab-injected EW-fed mice (Fig. 8h, i). However, bone loss was only slightly inhibited by αIL-4 mAb treatment (Fig. 8j), and at 28 days BV/TV, and BMC/TV were still significantly lower than in the controls ($P < 0.01$, CN-fed vs EW-fed control Ab-injected; $P < 0.05$, CN-fed vs EW-fed αIL-4 mAb-injected; Fig. 8k). Serum IL-4 levels did not differ among the three experimental groups (Fig. 8f, l), indicating that the effects of IL-4 occurred not systemically but locally. Thus, the bone loss observed in EW-fed OVA23-3 mice was triggered by activation of, and IL-4 production by, MLN $CD4^+$T cells and occurred IL-4 dependently in the primary phase of inflammation (until day 9 of EW feeding), whereas in the chronic phase the contribution of IL-4 dominance to bone-loss induction was lower.

To examine IL-4 production by $CD4^+$T cells and the effect of IL-4 dominance on bone loss, we first performed intracellular IL-4 staining of BM cells. $CD4^+$T cells of EW-fed R23-3/BALB mice secreted IL-4 in BM at similar levels on days 9 and 28 (Fig. S16). These results suggested that $CD44^{hi}CD62L^{lo}CD4^+$T cells (accounting for more than 60% of BM $CD4^+$T cells) produced IL-4 (Figs. 2a and S12). However, unlike in MLNs, in the BM other lymphoid cells produced more IL-4 than did $CD4^+$T cells (Fig. S16). To confirm the bone-loss-inducing roles of activated T cells, we injected RE2 mAb, which causes the death of activated T cells (resting T cells are insensitive)[27], into EW-fed R23-3 mice on days 0, 3, 6, and 9. Parameters (BV/TV, BMC, BMC/TV) of bone metabolism were significantly higher in RE2-mAb-injected EW-fed mice than in

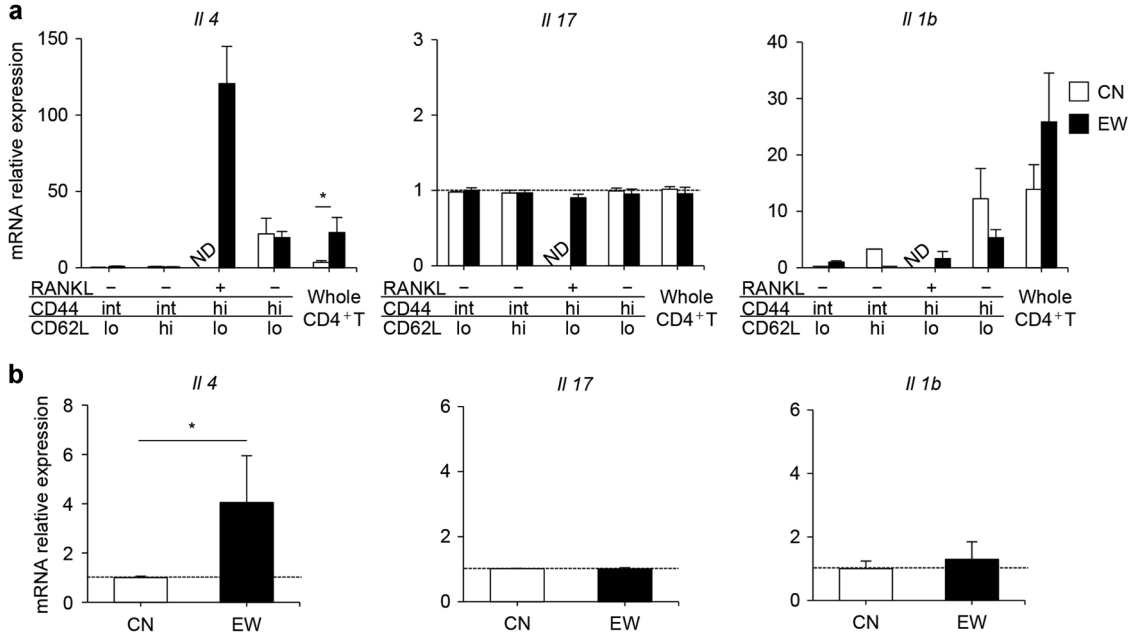

Fig. 7 Activated CD44^{hi}CD62L^{lo}CD4^{+}T cells in mesenteric lymph nodes (MLNs) show predominant IL-4 expression. Cytokine mRNA expression levels for MLN CD4^{+}T-cell subsets relative to those the values for the RANKL^{-}CD44^{int}CD62L^{hi}CD4^{+}T cells from CN-fed mice (horizontal line) (**a**) and all MLN cells relative to those for CN-fed mice (horizontal line) (**b**). + or −, positive or negative expression of RANKL molecule on CD4^{+}T-cell surface. Values were derived from OVA23-3 mice fed a CN or egg-white (EW) diet for 28 days were determined by Quantitative real-time RT-PCR. Data are representative of two independent experiments; $n = 2$ to 5 per experiment. ND = not detected. *$P < 0.05$ (EW vs. CN).

untreated (saline) EW-fed mice (Fig. S17), showing that OVA-activated T cells affected bone loss, as suggested by the slight recovery from bone loss in αIL-4 mAb-injected mice (Fig. 8). To clarify the direct effect of IL-4 dominance on osteoclast differentiation, we confirmed that IL-4 was below the ELISA detection limit in the supernatant of in vitro co-culture of preosteoclasts and CD4^{+}T cells (data not shown). We then found that adding IL-4 in in vitro culture inhibited osteoclast differentiation, although TRAP^{+}cells were observed in the same in vitro conditions upon co-culture of preosteoclasts and IL-1β in addition to IL-4 (Fig. S18). Thus, in this model, IL-4-producing aberrant activated CD4^{+}T cells from MLNs can migrate to BM and trigger osteoclast differentiation, helping to create the IL-4-induced inflammatory milieu[25].

DISCUSSION

We analyzed the immunological mechanism of bone loss after food-allergic enteropathy development in OVA23-3 mice. We found a specific relationship between MLNs and bone via IL-4 dominance created by OVA-specific Th2 cells in this comorbidity triggered by food-allergen intake. We can describe our model's mechanism of bone loss from two perspectives: the role of the immune responses in MLNs and the role of excessive IL-4 production in the lymphoid organs.

Comparison of the results obtained after mesenteric lymphadenectomy and after splenectomy (see Fig. 3), and analysis of cell migration from MLNs to BM (see Figs. 5 and S12), revealed a specific relationship between MLNs and bone. These results showed that MLNs, which orchestrate severe enteropathy as a central inflammatory lesion[5], were directly and IL-4-dependently connected with bone inflammatory responses, at least during the primary phase (until day 9, see Fig. 8). However, the spleen's immune responses differed from those in MLNs and BM, although these lymphoid organs were equally triggered by specific T-cell responses against OVA (Fig. 2a)[5]. The numbers of CD44^{hi}CD62L^{lo}CD4^{+}T cells as an EM phenotype were associated with these relationships (see Fig. 3c, e). These T cells, excessively activated by orally administered OVA, can easily migrate to BM and promote bone damage (see Figs. 4 and 5). However, in the chronic phase, in which there was recovery from severe enteropathy and weight loss in this model (Fig. 8h)[3,6], bone loss continued with only slight regulation by IL-4 (Fig. 8j, k, as shown by the lack of significant difference between αIL-4 mAb-treated and untreated EW-fed R23-3/BALB mice at day 28), contrary to the enteropathy and with the induction of forkhead box p3 (Foxp3)$^{+}$T cells in both the MLNs and spleen[6]. This suggests that the relationship among the lymphoid organs (MLNs, spleen, and BM) may change in the chronic phase (see Fig. S13). The intestinal state termed a "leaky gut,"[28,29] in which gut mucosal permeability increases, leading to the development of certain diseases (i.e., IBD), may promote bone loss continuation via immune responses as a specific gut–bone axis relationship in the chronic phase.

A previous study showed that almost 90% of Foxp3^{+}T cells in MLNs in 28-day EW-fed R23-3 mice express the CD44^{hi}CD62L^{lo} molecule[6]. Recent studies of T-cell roles[30] show that Foxp3^{+}Treg cells are important contributors to osteoclastogenesis inhibition via cytokines or CTLA-4 (cytotoxic T-lymphocyte-associated protein 4)[31], and intestinal bacterial metabolites induce Foxp3^{+}Treg cells and contribute to bone health in the gut–bone axis[32]. However, we found that MLN CD44^{hi}CD62L^{lo}CD4^{+}T cells have an inflammatory EM phenotype and induce osteoclastogenesis, despite long-term EW-feeding-induced dampening of the inflammatory response. Therefore, in our model, MLN EM T cells may change their characteristics (i.e., lose their Foxp3 expression and gain inflammatory ability) after migrating to BM, as suggested by the roles of exFoxpTh17 transdifferentiated into Th17[21,22]. In light of the strong IL-4-production abilities of EM T cells activated in MLNs in enteropathy, we found that these cells were involved in triggering and maintaining bone loss via unknown molecules or mediators (see Fig. S11) by creating IL-4 dominance in BM (Figs. S15 and S16)

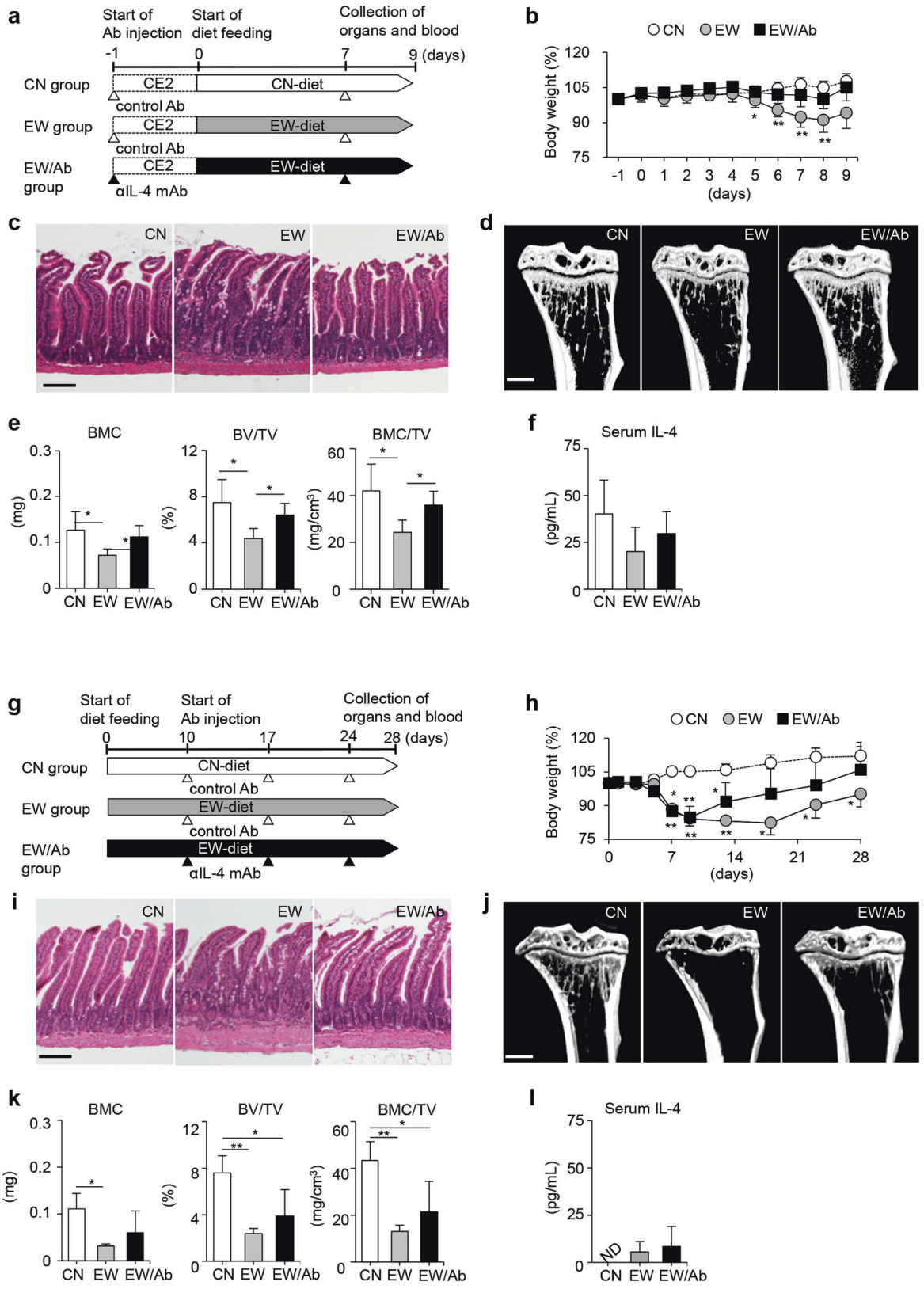

although they may merely migrate into BM as memory cells to enhance protection against continuous invasion by OVA[25].

Our findings suggested that excessive IL-4 production, inducing bone loss, occurred not via changes in serum IL-4 levels (see Fig. 8f, l), but locally and through the migration of IL-4-producing cells from MLNs to bone (Fig. S14) or through IL-4 production by resident BM cells (lymphocytes other than $CD4^+$cells, Figs. 6b and S16). Several reports have demonstrated the roles of IL-4 in bone

Fig. 8 Neutralization of IL-4 prevents weight loss, intestinal changes, and bone loss in R23-3/BALB mice. a, **g** Protocols for injection of anti-IL-4 monoclonal antibody (αIL-4 mAb) into R23-3/BALB mice before feeding of the egg-white (EW) diet and on day 7 of the diet (**a**) or after 10 days of EW feeding and on days 17 and 24 of the diet (**g**). At the end of each experimental period, mice were dissected and their tissues and serum samples were collected. **b**, **h** Time course of body-weight relative to initial weight (100%). Initial body weights were: for CN mice, 27.50 ± 1.55 g; EW mice, 27.73 ± 0.71 g; EW/Ab mice, 27.73 ± 1.11 g (**b**). Initial body weights were: for CN mice, 27.23 ± 1.79 g; EW mice, 27.43 ± 1.52 g; EW/Ab mice, 27.48 ± 0.44 g (**h**). **c**, **i** Hematoxylin-and-eosin-stained paraffin-embedded small intestinal tissues (4 μm thick) at day 9 (**c**) and day 28 (**i**). Scale bar = 100 μm. **d**, **j** Right tibia scanned by micro-computed tomography at day 9 (**d**) and day 28 (**j**). Scale bar = 1 mm. **e**, **k** Trabecular bone mineral content (BMC) of the tibia (left), bone volume/bone tissue (BV/TV, center), and BMC/TV (right) at day 9 (**e**) and day 28 (**k**). **f**, **l** Serum IL-4 levels were measured at day 9 (**f**) and day 28 (**l**). Values are expressed as means ± SD. CN, control-diet-fed control-Ab-injected mice; EW, EW-fed control-Ab-injected mice; EW/Ab, EW-fed αIL-4-mAb-injected mice. Data are representative of two independent experiments; $n = 6$ in each group (**a**–**e**), $n = 3$ in each group (**f**), $n = 4$ in each group (**g**–**l**). *$P < 0.05$ and **$P < 0.01$ (CN or EW/Ab vs. EW). ND = not detected.

loss in arthritis mouse models[33–35] or *lck*-IL-4 transgenic mice[10]; IL-4-deficient mice are less prone to the induction of autoantibody-mediated pathogenesis in arthritis, or to continuous IL-4 production in the osteoporosis that develops with decreased osteoblast activity in *lck*-IL-4 transgenic mice. Although the importance of IL-4-dependent bone loss in our mouse model is the same as in other arthritic mice[33–35] or *lck*-IL-4 transgenic mice[10], our model has some unique characteristics. In our system of non-IgE food-allergic enteropathy, allergen (OVA) intake clearly triggered an inflammation chain by internally penetrating the body via the gut mucosa and PPs and activating aberrantly Th2-dominant OVA-specific T cells in MLNs. Therefore, unexpectedly, the roles of MLNs were prominent in inducing bone loss, and a specific gut–bone axis relationship was induced via IL-4-producing cells in MLNs. However, the precise mechanism of IL-4-dependent bone-loss induction remains unclarified because of contradictory views on IL-4 function in bone metabolism[36–38]. IL-4/IL-13 reportedly promotes IL-6 production by osteoblasts synergistically with IL-1, a pro-inflammatory cytokine that promotes osteoclast differentiation[39] and bone loss[38]. However, IL-4 inhibits osteoclast formation by targeting osteoblasts or osteoclasts[30,40,41]. Our analysis also showed both an inhibitory effect of IL-4 and a promoting effect of IL-1β in combination with IL-4 on induction of TRAP$^+$multinucleated cells (see Fig. S18). The mechanism by which IL-4 production influences bone loss, including in relation to molecules or components other than specific cytokines or RANKL, needs to be examined further in detail. In non-IgE-mediated gastrointestinal food allergy, which has recently increased in prevalence worldwide, patients' milk-protein-stimulated peripheral blood mononuclear cells show a predominant Th2-skewing phenotype, as in our model[42]. In gastrointestinal food-allergy patients, excessive intestinal T-cell activation may influence bone metabolism. Our study provides new insights into the roles of activated lymphocytes in intestinal lymphoid tissues and other extraintestinal lymphoid organs—notably BM—in response to food allergens.

METHODS

Mice and diets

OVA23-3 mice were generated by isolation of genomic fragments encoding TCR-α and -β from OVA-specific I-A^d restricted CD4$^+$T cell clone 7-3-7[43]. Offspring with an H-2^d genetic background was produced from a mouse carrying transgenes by back-crossing with BALB mice. F1 mice were generated by crossing OVA23-3 mice with BALB mice, to attenuate allergen-specific responses to OVA. The other mice and diets used, and the ethical animal care, are described in Supplementary Information.

OVA administration to a different mice model of food-allergic enteropathy

Six- to 12-week-old mice (OVA23-3, R23-3, RD10, SR23-3, K23-3, R23-3/BALB, and BALB/ALUM) were fed experimental diets (CN or EW). R23-3/BALB mice were used for αIL-4 mAb treatment. R23-3 mice were used to purify OVA-specific CD4$^+$T cells and for RE2 mAb (rat anti-mouse pan-MHC class I mAb, provided by S. Matsuoka, Juntendo University)[27] treatment. For details of the establishment of the other experimental systems see Supplementary Information.

At the end of the experimental period, mice were euthanized by cervical dislocation and dissected to collect serum, bone, jejunum, lymphoid organs (PPs, MLNs, spleen, and sDLNs), and BM for further analysis. Single-cell suspensions from PPs, MLNs, spleen, and BM whole cells were prepared, and cells were purified by using magnetic-activated cell sorting[3,4]. Serum biomarkers to indicate health status of mice were analyzed. Tibias and femurs were analyzed by using micro-computed tomography (RmCT, Rigaku, Tokyo, Japan) and 3D bone morphology software (TRI/3D-BON; Ratoc, Tokyo, Japan) as described previously[44]. For bone histological analysis, the left femur was fixed with 70% ethanol and embedded in methylmethacrylate resin, and tissue sections (5 μm) were stained with Villanueva bone stain. For histology, longitudinal sections of jejunum (3 cm) were taken, fixed with 10% formalin, and embedded in paraffin. Sections 4 μm thick were stained hematoxylin and eosin. For details see Supplementary Information.

Flow cytometry

Single-cell suspensions prepared from PPs, MLNs, spleen, and BM whole cells were stained and analyzed as described previously[4–6]. Staining was performed with mAbs (see Supplementary Information). Cell-surface-expressed molecules were analyzed with a BD FACS Canto II and Verse flow cytometer (BD Biosciences, Franklin Lakes, NJ) and then evaluated with FlowJo (Tree Star, Ashland, OR) and FACS Diva software (BD Biosciences). Data were acquired at >100 counts for target cells.

Assessment of bone-damaging abilities of CD4$^+$T-cell subsets via osteoclasts

Preosteoclasts were prepared as described previously from BM cells isolated from 8-week-old male BALB mice (CLEA Japan Inc., Shizuoka, Japan)[44]. Preosteoclasts (3×10^4 cells/well) were placed on dentin slices (Wako Pure Chemical Corporation, Osaka, Japan) in a 96-well plate at 37 °C for 24 h. Purified MLN-CD4$^+$T-cell subsets (1×10^5 cells/well) were added to each well in the presence of 10 ng/mL RANKL (R&D Systems Minneapolis, MN) and 25 ng/mL M-CSF (macrophage colony-stimulating factor, R&D Systems). On day 12 of incubation, the cells were washed away and resorption pits were stained with Meyer's hematoxylin (Wako Pure Chemicals Corporation). Pit area was calculated by using Photoshop CS4 version 11.0 (Adobe Systems Inc., San Jose, CA) and ImageJ version 1.42 (NIH, Bethesda, MD). The osteoclastogenesis-induction ability of membrane-bound RANKL from CD44^{hi}CD62L^{lo}CD4$^+$ T cells was assessed by using an in vitro method similar to the pit formation assay but without the dentin slice and soluble RANKL added (see Supplementary Information). Recombinant IL-4 (0, 10 ng/mL, PeproTech, Cranbury, NJ) or recombinant IL-1β (0, 10 ng/mL, R&D Systems), were added at the time of addition of RANKL and M-CSF to induce directly osteoclastogenesis from BM cells.

Assessment of MLN CD44^{hi}CD62L^{lo}CD4$^+$T cell migration to BM in KikGR mice

KikGR mice[20] systemically express KikGR fluorescent protein, which is photoconverted from green to red when irradiated with violet light. Seven- to 10-week-old male K23-3 mice were prepared by crossing OVA23-3 and KikGR mice and fed a CN or EW diet for 9 days. Their MLNs were exposed surgically and irradiated with violet light (3 min per each of three sections of each MLN, 435-nm LED; Prizmatix, Holon, Israel) under isoflurane-induced anesthesia (Pfizer, New York, NY). On day 10, the mice were

dissected to collect the right tibia, small intestine, lymphoid organs (PPs, MLNs, spleen, and sDLNs), and BM for further analysis.

Quantitative real-time RT-PCR measurement of cytokine mRNA expression

Measurements of mRNA expression are described in Supplementary Information.

Inhibition of IL-4 or CD4$^+$T cells in EW-fed R23-3/BALB or R23-3 mice

R23-3/BALB mice were given αIL-4 mAb (1 mg per injection; clone 11B11, Bio X Cell, West Lebanon, NH) intravenously every 7 days (the first injection was one day before the start or on day 10). As a control, InVivoMAb Polyclonal Mouse IgG (1 mg/injection, Bio X Cell) was used. Body weights were measured every day. RE2 mAb was injected intraperitoneally into R23-3 mice fed an EW diet. At the end of the experiment, serum and tissues were taken for further analysis. (see Supplementary Information). Jejunal sections (for intestinal histology; hematoxylin and eosin-stained)[3], and bones (for micro-computed tomography analysis and flow cytometry) were taken for further analysis.

Intracellular IL-4 staining

BM cells were prepared from R23-3/BALB mice fed a CN or EW diet for 9 or 28 days. BM cells were resuspended at 2.5×10^6 cells/2 mL in complete RPMI 1640 with 10% fetal calf serum and stimulated with the activation regents ionomycin (2 μg/mL, Sigma-Aldrich, St. Louis, MO), phorbitol myristate acetate (10 ng/mL, Sigma-Aldrich), and brefeldin A (40 μg/mL, Sigma-Aldrich) in 48-well flat-bottomed plates (Falcon, New York, NY) at 37 °C for 4 h. After blocking with anti-CD16/CD32 mAb (BioLegend, San Diego, CA), the cells were stained with APC- or FITC-anti-mouse CD4 mAb (GK1.5, Biolegend) and Fixable Viability Dye eFluor 780 (FVD-eFlour780; eBioscience, Waltham, MA). Intracellular IL-4 was stained with PE- anti-mouse IL-4 mAb (11B11, BioLegend) by using a Flow Cytometry Fixation and Permeabilization Buffer Kit I (R&D Systems) and analyzed with BD FACSVerse (BD Biosciences).

Statistical analysis

For details of the statistical analysis see Supplementary Information.

REFERENCES

1. Amarasekara, D. S., Yu, J. & Rho, J. Bone loss triggered by the cytokine network in inflammatory autoimmune diseases. *J. Immunol. Res.* **2015**, 832127 (2015).
2. Ashcroft, A. J. et al. Colonic dendritic cells, intestinal inflammation, and T cell-mediated bone destruction are modulated by recombinant osteoprotegerin. *Immunity* **19**, 849–861 (2003).
3. Nakajima-Adachi, H. et al. Food antigen causes TH2-dependent enteropathy followed by tissue repair in T-cell receptor transgenic mice. *J. Allergy Clin. Immunol.* **117**, 1125–1132 (2006).
4. Ono-Ohmachi, A., Nakajima-Adachi, H., Morita, Y., Kato, K. & Hachimura, S. Milk basic protein supplementation exerts an anti-inflammatory effect in a food-allergic enteropathy model mouse. *J. Dairy Sci.* **101**, 1852–1863 (2017).
5. Nakajima-Adachi, H. et al. Peyer's patches and mesenteric lymph nodes cooperatively promote enteropathy in a mouse model of food allergy. *PLoS ONE* **9**, 2–11 (2014).
6. Nakajima-Adachi, H. et al. Critical role of intestinal interleukin-4 modulating regulatory T cells for desensitization, tolerance, and inflammation of food allergy. *PLoS ONE* **12**, 1–19 (2017).
7. Gatti, D. et al. Allergy and the bone: unexpected relationships. *Ann. Allergy Asthma Immunol.* **107**, 202–206 (2011).
8. Arima, K. et al. Burden of atopic dermatitis in Japanese adults: analysis of data from the 2013 National Health and Wellness Survey. *J. Dermatol.* **45**, 390–396 (2018).
9. Wu, C. Y. et al. Osteoporosis in adult patients with atopic dermatitis: a nationwide population-based study. *PLoS ONE* **12**, e0171667 (2017).
10. Lewis, D. B. et al. Osteoporosis induced in mice by overproduction of interleukin 4. *Proc. Natl Acad. Sci. USA* **90**, 11618–11622 (1993).
11. Burggraf, M. et al. Oral tolerance induction does not resolve gastrointestinal inflammation in a mouse model offoodallergy. *Mol. Nutr. Food Res.* **55**, 1475–1483 (2011).
12. Nakajima-Adachi, H. et al. Two distinct epitopes on the ovalbumin 323-339 peptide differentiating CD4+T cells into the Th2 or Th1 phenotype. *Biosci. Biotechnol. Biochem.* **76**, 1979–1981 (2012).
13. Kanai, T. et al. Naturally arising CD4+CD25+ regulatory T cells suppress the expansion of colitogenic CD4+CD44highCD62L−effector memory T cells. *Am. J. Physiol. Gastrointest. Liver Physiol.* **290**, G1051–1058 (2006).
14. Nemoto, Y. et al. Bone marrow retaining colitogenic CD4+ T cells may be a pathogenic reservoir for chronic colitis. *Gastroenterology* **132**, 176–189 (2007).
15. Nemoto, Y. et al. Long-lived colitogenic CD4+ memory T cells residing outside the intestine participate in the perpetuation of chronic colitis. *J. Immunol.* **183**, 5059–5068 (2009).
16. Rosa, F. D. & Santoni, A. Memory T-cell competition for bone marrow seeding. *Immunology* **108**, 296–304 (2003).
17. Rosa, F. D. & Pabst, R. The bone marrow: A nest for migratory memory T cells. *Trends Immunol.* **26**, 360–366 (2005).
18. Tokoyoda, K. et al. Professional memory CD4+ T lymphocytes preferentially reside and rest in the bone marrow. *Immunity* **30**, 721–730 (2009).
19. Kikuta, J. et al. Dynamic visualization of RANKL and Th17-mediated osteoclast function. *J. Clin. Invest.* **123**, 866–873 (2013).
20. Nakanishi, Y. et al. Regulatory T cells with superior immunosuppressive capacity emigrate from the inflamed colon to draining lymph nodes. *Mucosal Immunol.* **11**, 437–448 (2018).
21. Tsukasaki, M. et al. Host defense against oral microbiota by bone-damaging T cells. *Nat. Commun.* **9**, 701 (2018).
22. Komatsu, N. et al. Pathogenic conversion of Foxp3+ T cells into TH17 cells in autoimmune arthritis. *Nat. Med.* **20**, 62–68 (2013).
23. Sato, K. et al. Th17 functions as an osteoclastogenic helper T cell subset that links T cell activation and bone destruction. *J. Exp. Med.* **203**, 2673–2682 (2006).
24. Ciucci, T. et al. Bone marrow Th17 TNFα cells induce osteoclast differentiation, and link bone destruction to IBD. *Gut* **64**, 1072–1081 (2015).
25. Collins, N. et al. The bone marrow protects and optimizes immunological memory during dietary restriction. *Cell* **178**, 1088–1101 (2019).
26. Sugiyama, T., Omatsu, Y. & Nagasawa, T. Niches for hematopoietic stem cells and immune cell progenitors. *Int. Immunol.* **31**, 5–11 (2019).
27. Matsuoka, S. et al. A novel type of cell death of lymphocytes induced by a monoclonal antibody without participation of complement. *J. Exp. Med.* **181**, 2007–2015 (1995).
28. Schepper, J. D. et al. Probiotic *Lactobacillus reuteri* prevents postantibiotic bone loss by reducing intestinal dysbiosis and preventing barrier disruption. *J. Bone Miner. Res.* **34**, 681–698 (2019).
29. Mu, Q., Kirby, J., Reilly, C. M. & Luo, X. M. Leaky gut as a danger signal for autoimmune diseases. *Front. Immunol.* **8**, 598 (2017).
30. Srivastava, R. K., Dar, H. Y. & Mishra, P. K. Immunoporosis: Immunology of osteoporosis-role of T cells. *Front. Immunol.* **9**, 657 (2018).
31. Bozec, A. & Zaiss, M. M. T Regulatory cells in bone remodelling. *Curr. Osteoporos. Rep.* **15**, 121–125 (2017).
32. Zaiss, M. M., Jones, R. M., Schett, G. & Pacifici, R. The gut-bone axis: how bacterial metabolites bridge the distance. *J. Clin. Invest.* **129**, 3018–3028 (2019).
33. Svensson, L., Nandakumar, K. S., Johansson, Å., Jansson, L. & Holmdahl, R. IL-4-deficient mice develop less acute but more chronic relapsing collagen-induced arthritis. *Eur. J. Immunol.* **32**, 2944–2953 (2002).
34. Nandakumar, K. S. & Holmdahl, R. Arthritis induced with cartilage-specific antibodies is IL-4-dependent. *Eur. J. Immunol.* **36**, 1608–1618 (2006).
35. Ohmura, K., Nguyen, L. T., Locksley, R. M., Mathis, D. & Benoist, C. Interleukin-4 can be a key positive regulator of inflammatory arthritis. *Arthritis Rheum.* **52**, 1866–1875 (2005).
36. Yang, D. H. & Yang, M. Y. The role of macrophage in the pathogenesis of osteoporosis. *Int. J. Mol. Sci.* **20**, 2093 (2019).
37. Pereira, M. et al. Common signalling pathways in macrophage and osteoclast multinucleation. *J. Cell Sci.* **131**, jcs216267 (2018).
38. Silfverswärd, C. J., Frost, A., Brändström, H., Nilsson, O. & Ljunggren, Ö. Interleukin-4 and interleukin-13 potentiate interleukin-1 induced secretion of interleukin-6 in human osteoblast-like cells. *J. Orthop. Res.* **22**, 1058–1062 (2004).
39. Nakamura, I. & Nakamura, I. Regulation of osteoclast differentiation and function by interleukin-1. *Vitam. Horm.* **74**, 357–370 (2006).
40. Amarasekara, D. S. et al. Regulation of osteoclast differentiation by cytokine networks. *Immune Netw.* **18**, e8 (2018).
41. Yamada, A. et al. Interleukin-4 inhibition of osteoclast differentiation is stronger than that of interleukin-13 and they are equivalent for induction of production from osteoblasts. *Immunology* **120**, 573–579 (2007).
42. Morita, H. et al. Food protein-induced enterocolitis syndromes with and without bloody stool have distinct clinicopathologic features. *J. Allergy Clin. Immunol.* **140**, 1718–21 (2017).
43. Sato, T. et al. Naive T cells can mediate delayed-type hypersensitivity response in T cell receptor transgenic mice. *Eur. J. Immunol.* **24**, 1512–6 (1994).

44. Ono-Ohmachi, A., Ishida, Y., Morita, Y., Kato, K. & Nara, T. Y. Milk basic protein facilitates increased bone mass in growing mice. *J. Nutr. Sci. Vitaminol. (Tokyo)* **63**, 315–322 (2017).

ACKNOWLEDGEMENTS

We thank Erika Hiraide, Mamiko Morinaga, Tomiko Asakura, Takashi Matsuwaki, Yoshikazu Saito, Takuya Miyakawa, and Jun Kunisawa (the University of Tokyo); staff of the Institute of Medical Science and the FACS Core Laboratory at the University of Tokyo; Naoyuki Takahashi (Matsumoto Dental University); Ken Kato, Atsushi Serizawa, and Takayuki Nara (Megmilk Snow Brand Co., Ltd.); Toshimitsu Yoshioka and Takashi Fujita (Bean Stalk Snow Co., Ltd.); and Akemi Ito (Ito Bone Histomorphometry Institute) for their technical advice and support.

AUTHOR CONTRIBUTIONS

H.N.A. and A.O.O. provided substantial contributions to the conception of the work. M.T. provided KikGR mice. S.K. and Y.I. provided recombinant IL-1β and S.M. provided RE2 mAb and performed experiments. N.U., Y.N. and M.K. helped with the analysis of the bone. A.O.O., H.N.A., S.Y., S.U., M.T., K.S., S.N., Y.M., T.T., and T.I. performed the experiments and analyzed the data. H.N.A. and A.O.O. wrote the manuscripts. All authors discussed and interpreted the data.

COMPETING INTERESTS

This work was supported by grants from the Kieikai Research Foundation (H.N.A., 2017S063, 2018T019), a Grant-in-Aid for Scientific Research (C) (H.N.A., 18K05502) from the Japan Society for the promotion of science, a grant from The Food Science Institute Foundation (Ryoushoku-kenkyukai; H.N.A., No. 2019A01), and grants from Megmilk Snow Brand Co., Ltd. (H.N.A., H.K., and S.H.). The authors declare no conflict of interest associated with this manuscript.

ADDITIONAL INFORMATION

Supplementary information The online version contains supplementary material available at https://doi.org/10.1038/s41385-021-00434-2.

Correspondence and requests for materials should be addressed to H.N.-A.

Reprints and permission information is available at http://www.nature.com/reprints

Publisher's note Springer Nature remains neutral with regard to jurisdictional claims in published maps and institutional affiliations.